

# Circumstellar disks around Herbig Ae/Be stars: polarization, outflows and binary orbits

G. Maheswar, P. Manoj and H. C. Bhatt

Indian Institute of Astrophysics, Bangalore 560 034, India

**Abstract.** The geometrical relationship between the distribution of circumstellar matter, observed optical linear polarization, outflows and binary orbital plane in Herbig Ae/Be stars is investigated. Optical linear polarization measurements carried out for a number of Herbig Ae/Be stars that are either known to be in binary systems and/or have bipolar jets are presented in this paper. Available information on the position angles of polarization, outflows and binary companions for Herbig Ae/Be stars is compiled and analysed for any possible correlations. In  $\approx 85\%$  of the sources the outflow position angle is within  $30^\circ$  of being parallel or perpendicular to the polarization position angle. In  $\approx 81\%$  of the sources the binary position angle is within  $30^\circ$  of being parallel or perpendicular to the polarization position angle. Out of 15 sources with bipolar outflows, 10 sources have the binary position angle within  $30^\circ$  of being perpendicular to the outflow position angle. These results favour those binary formation mechanisms in which the binary components and the disks around individual stars or circumbinary disks are coplanar.

**Key words:** Stars: pre-main sequence - binaries:general - circumstellar matter - ISM: jets and outflows - polarization - scattering

## 1. Introduction

Herbig Ae/Be stars are pre-main sequence (PMS) objects of intermediate mass ( $2 \leq M/M_\odot \leq 8$ ). In the original survey (Herbig 1960) these objects were defined as A and B stars, located in regions of known star formation, with emission in the Balmer lines of hydrogen and associated with optical reflection or emission nebulosity. Herbig (1960) listed 26 objects belonging to this class. The catalogue was later expanded by Finkenzeller & Mundt (1984) to include 57 stars. The most recent catalogue by

Thé et al. (1994), adopting a more extended definition, lists 109 Herbig Ae/Be stars and a number of candidates that include stars with later spectral types (G0 or earlier) and those found relatively isolated from star forming clouds. The PMS nature of Herbig Ae/Be stars is now well established, based on their position in the HR diagram and comparison with theoretical evolutionary tracks (Strom et al. 1972; Cohen & Kuhi 1979; van den Ancker et al. 1998; Palla & Stahler 1991). Infrared, submillimetre and millimetre measurements have shown that Herbig Ae/Be stars are associated with significant amounts of circumstellar dust emitting excess radiation, over that produced by stellar photosphere, at these wavelengths (eg., Rydgren et al. 1976; Cohen & Kuhi 1979; Bertout et al. 1988; Strom et al. 1988; Beckwith et al. 1990; Weintraub Sadnell & Duncan 1989; Adams et al. 1990; Hillenbrand et al. 1992). The existence of circumstellar dust is also supported by the relatively large values of intrinsic polarization observed for these objects (eg., Breger 1974; Garrison & Anderson 1978; Vrba et al. 1979; Jain et al. 1990; Jain & Bhatt 1995; Yudin & Evans 1998) which is generally ascribed to the presence of circumstellar dust grains (eg., Bastien 1987).

While the existence of circumstellar dust around Herbig Ae/Be stars is well established, the geometrical distribution of the dust is not yet fully clear. Hillenbrand et al. (1992), from an analysis of the spectral energy distributions (SED) of 47 Herbig Ae/Be stars, classified these objects into three groups. The infrared SED of the Group I objects ( $\lambda F_\lambda \sim \lambda^{-4/3}$ ) could be explained by invoking a geometrically thin, optically thick circumstellar accretion disk with an optically thin inner region to account for the observed inflections in their near-infrared spectra. Group II objects, with flat or rising infrared spectra, consist of a star or star/disk system surrounded by gas and dust that is not confined to a disk. Group III objects have small or no infrared excess, similar to classical Be stars, and the small excesses can be ascribed to free-free emission in a gaseous envelope. Berrilli et al. (1992), on the other hand, produced models with spherically symmetric dust envelopes. Natta et al.

Send offprint requests to: G. Maheswar  
Correspondence to: maheswar@iiap.ernet.in,  
manoj@iiap.ernet.in, hcbhatt@iiap.ernet.in

(1993) proposed models with at least three components that contribute to the observed infrared emission: the central star, a circumstellar disk, and an extended, almost spherically symmetric, envelope. Models with symmetrical envelopes generally lead to much higher visual extinctions toward the central star than are observed.

Polarimetric measurements provide an important tool to study the nature and geometry of the circumstellar material. The integrated light from a Herbig Ae/Be object can have intrinsic polarization (in addition to the interstellar component) only if the distribution of the scattering material in its circumstellar regions is not spherically symmetric. Circumstellar dust distributed in a disk can cause relatively large polarization, the degree of polarization depending on the amount of scattering dust, degree of flattening of the disk and its orientation with respect to the observer's line of sight to the star. If the disk optical depth is small ( $\tau \leq 0.3$ ) and polarization is produced by single scattering, then the position angle of the  $E$  vector of the linearly polarized light is perpendicular to the disk, while for optically thick disks the observed polarization may be dominated by optically thin scattering dust distributed perpendicularly to the disk (for example in bipolar jets and outflows) resulting in a polarization position angle that is parallel to the disk plane (eg., Brown & McLean 1977; Elsasser & Staude 1978). Polarization vectors perpendicular to the disk plane can also be obtained for scattering off the surface of optically thick disks, while polarization vectors parallel to the disk plane require the addition of an extensive circumstellar envelope (see eg., Whitney & Hartmann 1992, 1993). Some Herbig Ae/Be stars, similarly to their lower mass counterparts, the T Tauri stars, have also been found to exhibit bipolar optical jets and molecular outflows (eg., Canto et al. 1984; Strom et al. 1986; Corcoran & Ray 1998) which are believed to be directed perpendicular to the circumstellar disks (eg. Konigl, 1982). One may therefore expect a correlation between the position angle of polarization and the direction of the jets and outflows from the Herbig Ae/Be stars. In a sample of 23 T Tauri stars and other young stellar objects, including 8 Herbig Ae/Be stars, Bastien (1987) found that for about 50 to 60 % of the sources the directions of the outflow and of the polarization are within  $30^\circ$  of being perpendicular to each other. If only the 8 Herbig Ae/Be stars in their sample are considered, then the correlation is not clear. In recent years more extensive polarization measurements and observations of jets and outflows from more Herbig Ae/Be stars have become available. A study of the correlation between the polarization and outflow directions can now be performed on a larger sample of Herbig Ae/Be stars.

A relatively large fraction (as compared with that for the main-sequence field stars) of Herbig Ae/Be stars

**Table 1.** Polarization of the observed Herbig Ae/Be stars.

| Object    | Date of observation | P (%) | $\theta_p$ ( $^\circ$ ) | $\epsilon_p$ (%) | $\epsilon_\theta$ ( $^\circ$ ) |
|-----------|---------------------|-------|-------------------------|------------------|--------------------------------|
| HD 35187  | 03 Mar 00           | 0.18  | 128                     | 0.07             | 8                              |
| GU CMa    | 10 Mar 99           | 1.19  | 28                      | 0.07             | 2                              |
| NX Pup    | 02 Mar 00           | 1.23  | 38                      | 0.23             | 6                              |
| Her 4636  | 01 Mar 00           | 0.77  | 157                     | 0.12             | 6                              |
| HD 141569 | 29 Apr 00           | 0.79  | 82                      | 0.05             | 1                              |
| HD 144432 | 30 Apr 00           | 0.47  | 20                      | 0.06             | 4                              |

have been found to have binary companions (eg., Leinert et al. 1997). Are the circumstellar (or circumbinary) disks in the binary Herbig Ae/Be systems coplanar with the binary orbital plane? Their relative orientations may depend on the binary formation process. For example, fragmentation of rotating protostellar clouds during collapse (eg. Boss 1988) to form binary systems will favour the formation of disks that are coplanar with the orbital plane. On the other hand, formation of the binary system by capture of independent young stellar or protostellar objects (eg., Larson 1990) will not favour any such alignment. An observational study of the relative orientations of the polarization position angles, bipolar outflows and binary orbital planes may therefore be useful in discriminating between the different models for the origin of binary systems.

In this paper we present the results of our measurements of optical linear polarization for a number of Herbig Ae/Be stars that are either known to be in binary systems and/or have bipolar jets. Available information on the position angles of polarization, outflows and binary companions for Herbig Ae/Be stars is compiled and analysed for any possible correlations. Our polarimetric observations are presented in Section 2. Data from the literature is compiled in Section 3. Various correlations are presented in section 4 and discussed in Section 5. Conclusions are summarized in Section 6.

## 2. Observations

Optical linear polarization measurements of 6 Herbig Ae/Be stars were made with a fast star and sky chopping polarimeter (Jain & Srinivasulu 1991) coupled at the  $f/13$  Cassegrain focus of the  $1m$  telescope at Vainu Bappu Observatory, Kavalur of the Indian Institute of Astrophysics. A dry-ice cooled R943-02 Hamamatsu photomultiplier tube was used as the detector. All measurements were made in the  $V$  band with an aperture of  $15arcsec$ . Observations were made during the period of 1999-2000. The instrumental polarization was determined by observing unpolarized standard stars from Serkowski (1974). It was found to be  $\sim 0.1\%$ , and has been subtracted vectorially from the observed polarization of the

programme stars. The zero of the polarization position angle was determined by observing polarized standard stars from Hsu & Breger (1982). The position angle is measured from the celestial north, increasing eastward. The Herbig Ae/Be stars selected for observations were taken from the Thé et al. (1994) catalogue. HD 35187 (Dunkin et al. 1998) and Her 4636 (Williams et al. 1977) satisfy all the criteria of being Herbig Ae/Be stars and hence we have made polarimetric observations of these objects and included them in our sample. The selected objects are either known to have outflows and/or are in binary systems. Results of our polarimetric measurements are given in Table 1. Columns in Table 1 give respectively, (1) identification of the star, (2) date of observation, (3) degree of polarization, (4) polarization position angle, (5-6)  $1\sigma$  probable errors in measurements of polarization and the position angle.

### 3. Data on polarization, outflows and binary companions of Herbig Ae/Be stars

In recent years several studies on polarization, outflows and binarity of Herbig Ae/Be stars have become available in the literature. In Table 2 we list position angle of the binary companion and outflow taken from the literature. The columns give, respectively, (1) object identification, (2-3) distance and spectral type taken from the literature, (4) secondary component position angle with respect to primary measured from celestial north, (5) angular separation (*arcsec*) of the secondary from the primary star, (6) derived projected linear separation (AU) of the secondary component from the primary star, (7) the mode of detection, (8) outflow position angle, (9) references. In Table 3 we list polarization data on Herbig Ae/Be stars. The column 1 gives object identification, columns 2 and 3 give observed degree of polarization and position angle. For most of the stars measurements at multiple epochs are available. Average values are given here. Columns 4 and 6 give estimated contribution of interstellar polarization and its position angle. Contributions to the observed polarization in young stellar objects are primarily due to the scattering of stellar light by dust distributed in the circumstellar environment and that due to the interstellar medium. For most of the Herbig Ae/Be stars being considered here, the observed polarization is dominated by the circumstellar component. The interstellar contribution becomes relatively more important for stars which have smaller circumstellar polarization either due to smaller quantities of scattering dust or due to unfavourable orientation, especially for more distant objects. We estimate the interstellar contribution to the polarization of the Herbig Ae/Be stars by considering the observed polarization of normal stars, at different distances in the direction of the object, from the catalogue Stellar polarization catalogs

agglomeration by Heiles (2000). Around each Herbig Ae/Be star, a search is made for normal stars in circles of increasing angular radii. Minimum of 10 stars are used to estimate the interstellar contribution to each target star. Circles of radius  $1^\circ$ ,  $2^\circ$ ,  $3^\circ$ ,  $5^\circ$  and  $7^\circ$  are used to choose the stars. If less than 10 stars are found in  $7^\circ$ , those stars are used. Stoke's parameters  $U$  ( $=P\sin 2\theta$ ) and  $Q$  ( $=P\cos 2\theta$ ) are evaluated from the degree of polarization ( $P$ ) and position angle ( $\theta$ ) for each star.  $U$  and  $Q$  parameters thus evaluated are plotted against the distance to the respective stars. Stoke's parameters  $U_{ism}$  and  $Q_{ism}$  representing interstellar polarization at the target star's distance are estimated by making a least-square fit. The interstellar polarization value  $P_{ism}$  and position angle  $\theta_{ism}$  are calculated as

$$P_{ism} = \sqrt{(U_{ism})^2 + (Q_{ism})^2}$$

$$\theta_{ism} = (1/2)\tan^{-1}(U_{ism}/Q_{ism})$$

$P_{ism}$  and  $\theta_{ism}$ , and probable errors  $\epsilon_{p_{ism}}$  and  $\epsilon_{\theta_{ism}}$  in their estimation, are given in columns 4, 6 and 5, 7 of Table 3 respectively. Stoke's parameters  $U_\star$  and  $Q_\star$  representing the observed polarization for the target stars are evaluated from the observed degree of polarization and position angle measured at each epoch. The Stoke's parameter  $U_i$  and  $Q_i$  representing the intrinsic (circumstellar polarization of the target star) polarization are estimated as

$$U_i = U_\star - U_{ism}$$

$$Q_i = Q_\star - Q_{ism}$$

The intrinsic polarization  $P_i$  and position angle  $\theta_i$  are then evaluated as

$$P_i = \sqrt{(U_i)^2 + (Q_i)^2}$$

$$\theta_i = (1/2)\tan^{-1}(U_i/Q_i)$$

In the case of V892 Tau, HD 150193 and Par 21 not many stars are available to determine the interstellar polarization and position angle. However, we note that they have relatively high observed polarization and are at relatively smaller distances. With relatively small intrinsic interstellar contribution, the observed polarization for the stars is considered to represent their intrinsic polarization in this study. Columns 8 and 9 give average values of intrinsic degree of polarization and position angle for Herbig Ae/Be stars corrected for the estimated interstellar contribution. Column 10 gives number of multiple epoch observations used for each star. Columns 11 and 12 give the probable errors in the polarization and position angle values inclusive of the dispersions in the individual measurements at different epochs. The

**Table 2.** Data on binarity and outflows in Herbig Ae/Be stars

| Object           | Dis.<br>(pc) | Sp.typ | $\theta_b$<br>( $^\circ$ ) | Angular<br>Separation<br>( <i>arcsec</i> ) | Linear<br>Separation<br>(AU) | Mode of<br>detection | $\theta_o$<br>( $^\circ$ ) | Ref     |
|------------------|--------------|--------|----------------------------|--|------------------------------|----------------------|----------------------------|---------|
| V633 Cas         | 600          | A5     | 3                          | 5.5  | 3300                         | Near Infrared (NIR)  | 160                        | 1,11    |
| V376 Cas         | 600          | F0     | -                          | -  | -                            | -                    | 120                        | 3       |
| XY Per           | 160          | B6     | 255                        | 1.2  | 192                          | NIR                  | -                          | 2       |
| V892 Tau         | 140          | A6     | 23                         | 4.1  | 570                          | NIR                  | -                          | 1       |
| UX Ori           | 460          | A2     | 257                        | 0.02                                       | 10                           | Optical              | -                          | 3       |
| HD 35187         | 150          | A2     | 185                        | 1.3  | 195                          | Optical              | -                          | 10      |
| CO Ori           | 460          | F8     | 280                        | 2.0  | 920                          | Optical              | -                          | 3       |
| HK Ori           | 460          | A5     | 42                         | 0.3  | 138                          | NIR                  | 160                        | 1,12    |
| T Ori            | 460          | B9     | 73                         | 7.7  | 3540                         | NIR                  | -                          | 1       |
| V380 Ori         | 460          | B9     | 204                        | 0.15                                       | 71                           | NIR                  | 56,149                     | 1,11    |
| LkH $\alpha$ 208 | 1000         | B7     | 114                        | 0.12                                       | 120                          | NIR                  | 0                          | 1,13    |
| GGD 18           | 1600         | B2     | 254                        | 5.8  | 9280                         | NIR                  | 150                        | 22,23   |
| R Mon            | 800          | B0     | 331                        | 0.7  | 560                          | NIR                  | 0                          | 4,11    |
| Gu CMa           | 1150         | B1     | 189                        | 0.7  | 800                          | Optical              | -                          | 5       |
| Z CMa            | 1150         | B5     | 123                        | 0.1  | 115                          | NIR                  | 60                         | 1,14    |
| HD 53367         | 240          | B0     | 298                        | 0.7  | 167                          | Optical              | -                          | 5       |
| NX Pup           | 500          | A0     | 62                         | 0.13                                       | 65                           | NIR                  | -                          | 6       |
| HD 76534         | 400          | B3     | 304                        | 2.0  | 800                          | Optical              | -                          | 5       |
| Her 4636         | 600          | B2     | 34                         | 3.3  | 1980                         | Optical              | 148                        | 9,20    |
| HD 141569        | 100          | A0     | 312                        | 6.8  | 680                          | NIR                  | -                          | 2       |
| HD 144432        | 250          | A7     | 354                        | 1.2  | 300                          | Optical              | -                          | 5       |
| HR 5999          | 200          | A0     | 115                        | 1.4  | 280                          | NIR                  | -                          | 1       |
| HD 150193        | 150          | A2     | 236                        | 1.1  | 165                          | NIR                  | -                          | 2       |
| KK Oph           | 160          | A6     | 247                        | 1.5  | 240                          | NIR                  | -                          | 1       |
| HD 163296        | 120          | A0     | -                          | -  | -                            | -                    | 8                          | 15      |
| AS 310           | 2500         | B0     | 153                        | 4.2  | 11000                        | NIR                  | 55                         | 7,12    |
| R CrA            | 130          | F0     | -                          | -  | -                            | -                    | 130                        | 13      |
| T CrA            | 130          | F5     | 275                        | 0.14                                       | 18                           | Optical              | 133                        | 8,13    |
| Par 21           | 400          | A5     | -                          | -  | -                            | -                    | 155                        | 21      |
| V1685 Cyg        | 1000         | B2     | 23                         | 0.14                                       | 141                          | Optical              | -                          | 5       |
| MWC 349          | 1200         | B[e]   | 280                        | 2.4  | 2880                         | Optical              | 10                         | 25      |
| LkH $\alpha$ 234 | 1000         | B3     | 315                        | 2.7  | 2700                         | NIR                  | 226,252                    | 1,18,21 |
| PV Cep           | 600          | A5     | -                          | -  | -                            | -                    | 348                        | 16      |
| HD 200775        | 400          | B2     | 164                        | 2.3  | 900                          | NIR                  | 70                         | 2,17    |
| AS 477           | 900          | A0     | 43                         | 4.2  | 3762                         | NIR                  | 112                        | 2,12    |
| LkH $\alpha$ 233 | 800          | A5     | -                          | -  | -                            | -                    | 50,90                      | 13      |
| HD 216629        | 725          | B2     | 147                        | 7.0  | 5046                         | NIR                  | -                          | 1       |
| MWC 1080         | 2500         | B0     | 86                         | 4.7  | 11725                        | NIR                  | 60                         | 1,19    |

Notes:

V380 Ori and LkH $\alpha$ 233 have two outflow components.

LkH $\alpha$ 234 shows an inner infrared jet at position angle 226 $^\circ$  and an outer optical jet at a position angle 252 $^\circ$  (Cabrit et al. 1997).

MWC 1080 is a triple systems consisting of a close unresolved spectroscopic binary and a tertiary star. Position angle of the tertiary is given here.

References

- 1) Leinert et al. 1997; 2) Pirzkal et al. 1997; 3) Bertout et al. 1999; 4) Close 1997; 5) Dommagnet 1994; 6) Brandner et al. 1995; 7) Ageorges et al. 1997; 8) Bailey J. 1998; 9) Chelli et al. 1995; 10) Dunkin et al. 1998; 11) Strom et al. 1986; 12) Goodrich 1993; 13) Bastien 1987; 14) Poetzal et al. 1989; 15) Devine et al. 2000; 16) Reipurth et al. 1997; 17) Watt 1986; 18) Ray et al. 1990; 19) Poetzal et al. 1992; 20) White 1993; 21) Cabrit et al. 1997; 22) Lenzen et al. 1984; 23) Lada and Gautier 1982; 24) Meyer et al. 2001; 25) White and Becker 1985.

**Table 3.** Data on polarization in Herbig Ae/Be stars

| Object           | $\langle P_\star \rangle$<br>(%) | $\langle \theta_\star \rangle$<br>( $^\circ$ ) | $P_{ism}$<br>(%) | $\epsilon_{P_{ism}}$<br>(%) | $\theta_{ism}$<br>( $^\circ$ ) | $\epsilon_{\theta_{ism}}$<br>( $^\circ$ ) | $\langle P_i \rangle$<br>(%) | $\langle \theta_i \rangle$<br>( $^\circ$ ) | n    | $\sigma_p$<br>(%) | $\sigma_\theta$<br>( $^\circ$ ) | Aperture<br>(arcsec) | Ref        |
|------------------|----------------------------------|--|------------------|-----------------------------|--------------------------------|---|------------------------------|--|------|-------------------|---------------------------------|----------------------|------------|
| (1)              | (2)                              | (3)  | (4)              | (5)                         | (6)                            | (7)                                       | (8)                          | (9)  | (10) | (11)              | (12)                            | (13)                 | (14)       |
| V633 Cas         | 1.67                             | 25   | 1.24             | 0.26                        | 72                             | 6   | 2.30                         | 9  | 3    | 0.26              | 10                              | 10,15,8.3            | 1,2        |
| V376 Cas         | 22.0                             | 26   | 1.22             | 0.26                        | 71                             | 6   | 23.5                         | 24   | 7    | 1.65              | 3                               | 10,15,8.3            | 1,2        |
| XY Per           | 1.58                             | 126  | 0.15             | 0.39                        | 140                            | 52  | 1.45                         | 124  | 7    | 0.07              | 3                               | 10,15                | 3,4        |
| V892 Tau         | 4.72                             | 3  | -                | -                           | -                              | -   | 4.72                         | 3  | 1    | 0.29              | 2                               | 12                   | 5          |
| UX Ori           | 1.22                             | 99   | 0.26             | 0.12                        | 123                            | 13  | 1.07                         | 94   | 10   | 0.21              | 7                               | 20,10                | 6,4        |
| HD 35187         | 0.18                             | 128  | 0.51             | 0.29                        | 61                             | 17  | 0.65                         | 145  | 1    | 0.07              | 8                               | 15                   | 15         |
| CO Ori           | 2.28                             | 164  | 0.17             | 0.39                        | 97                             | 52  | 2.39                         | 165  | 9    | 0.28              | 9                               | 4.3,10               | 10,4       |
| HK Ori           | 1.10                             | 159  | 0.08             | 0.35                        | 89                             | 52  | 1.17                         | 161  | 5    | 0.18              | 6                               | 10,15,-,13           | 1,3,7,8,9  |
| T Ori            | 0.32                             | 94   | 0.15             | 0.16                        | 148                            | 32  | 0.28                         | 100  | 11   | 0.10              | 40                              | 10,-,13              | 3,7,8,9,4  |
| V380 Ori         | 0.92                             | 88   | 0.16             | 0.19                        | 72                             | 35  | 0.80                         | 91   | 6    | 0.29              | 7                               | 15,-,14.3,20         | 3,7,8,11,6 |
| LkH $\alpha$ 208 | 2.28                             | 6  | 1.46             | 0.38                        | 172                            | 8   | 1.24                         | 25   | 4    | 0.49              | 11                              | 10,15,13,-           | 1,9,7,8    |
| GGD 18           | 3.60                             | 81   | -                | -                           | -                              | -   | 3.60                         | 81   | 1    | 0.50              | 2                               | -                    | 24         |
| R Mon            | 13.0                             | 92   | 0.70             | 0.34                        | 167                            | 14  | 13.5                         | 91   | 10   | 1.96              | 8                               | 26,8,13,15,10        | 12,1,8     |
| Gu CMa           | 1.25                             | 21   | 0.47             | 0.36                        | 146                            | 22  | 1.46                         | 29   | 4    | 0.07              | 4                               | 10,15                | 13,14,3,15 |
| Z CMa            | 0.80                             | 125  | 0.36             | 0.32                        | 135                            | 26  | 0.67                         | 173  | 5    | 0.26              | 23                              | 10,-,20,15           | 3,7,8,16   |
| HD 53367         | 0.53                             | 36   | 0.14             | 0.28                        | 152                            | 52  | 0.62                         | 41   | 2    | 0.04              | 1                               | 10,15                | 3,8        |
| NX Pup           | 1.10                             | 47   | 0.28             | 0.13                        | 38                             | 13  | 0.82                         | 50   | 2    | 0.21              | 10                              | 20,10                | 15,16      |
| HD 76534         | 0.61                             | 126  | 0.15             | 0.38                        | 88                             | 52  | 0.59                         | 133  | 1    | 0.29              | 11                              | 15                   | 3          |
| Her 4636         | 0.80                             | 159  | 0.12             | 0.06                        | 86                             | 14  | 0.90                         | 162  | 2    | 0.05              | 1                               | -,15                 | 22,15      |
| HD 141569        | 0.57                             | 88   | 1.00             | 0.71                        | 86                             | 20  | 0.43                         | 175  | 10   | 0.71              | 20                              | 15                   | 4,15       |
| HD 144432        | 0.30                             | 30   | 0.24             | 2.38                        | 36                             | 52  | 0.19                         | 172  | 5    | 2.39              | 52                              | 15                   | 4,15       |
| HR 5999          | 0.52                             | 177  | 0.96             | 0.62                        | 17                             | 19  | 0.68                         | 121  | 2    | 0.62              | 19                              | -                    | 29         |
| HD 150193        | 4.91                             | 59   | -                | -                           | -                              | -   | 4.91                         | 59   | 6    | 0.51              | 9                               | 15,12,20             | 3,4,5      |
| KK Oph           | 5.10                             | 180  | 0.13             | 0.26                        | 179                            | 52  | 4.92                         | 180  | 10   | 1.33              | 8                               | 20,10                | 16,4       |
| HD 163296        | 0.21                             | 59   | 0.70             | 0.45                        | 162                            | 19  | 0.76                         | 70   | 13   | 0.45              | 19                              | 15,13,27             | 3,17,18    |
| R CrA            | 7.6                              | 189  | 0.02             | 0.09                        | 31                             | 52  | 7.6                          | 9  | 1    | 0.50              | 5                               | 5                    | 21         |
| T CrA            | 4.59                             | 181  | 0.02             | 0.09                        | 31                             | 52  | 4.58                         | 1  | 3    | 2.86              | 11                              | 10,15,5              | 1,8,21     |
| Par 21           | 7.60                             | 75   | -                | -                           | -                              | -   | 7.60                         | 75   | 1    | 1.50              | 6                               | 7                    | 23         |
| V1685 Cyg        | 1.18                             | 14   | 0.16             | 0.46                        | 12                             | 52  | 1.02                         | 15   | 6    | 0.08              | 4                               | 15                   | 8,3,4      |
| MWC 349          | 7.70                             | 167  | 3.6              | 0.50                        | 100                            | 20  | 10.4                         | 174  | 11   | 1.55              | 4                               | -                    | 25,26      |
| LkH $\alpha$ 234 | 0.53                             | 107  | 0.87             | 0.65                        | 43                             | 21  | 1.16                         | 149  | 11   | 0.65              | 21                              | 10,15,13             | 1,9,8,4    |
| PV Cep           | 14.2                             | 77   | 0.99             | 0.50                        | 141                            | 15  | 14.8                         | 76   | 1    | 0.41              | 1                               | -                    | 19         |
| HD 200775        | 0.94                             | 93   | 0.69             | 0.52                        | 141                            | 21  | 1.23                         | 76   | 4    | 0.50              | 21                              | 10,15                | 1,7,8      |
| AS 477           | 1.10                             | 35   | 0.49             | 0.58                        | 35                             | 34  | 0.84                         | 44   | 5    | 0.41              | 42                              | 10,15,13,-           | 1,9,3,7,20 |
| LkH $\alpha$ 233 | 11.1                             | 156  | 0.60             | 0.78                        | 85                             | 37  | 11.6                         | 157  | 2    | 0.40              | 2                               | 10,15                | 1,8        |
| HD 216629        | 4.72                             | 105  | 1.29             | 0.67                        | 80                             | 15  | 4.03                         | 112  | 1    | 0.20              | 1                               | -                    | 27         |
| MWC 1080         | 2.00                             | 75   | 2.18             | 1.00                        | 72                             | 13  | 0.42                         | 150  | 10   | 1.00              | 30                              | 10,15,13,8.3         | 1,9,8,28   |

Notes:

GGD 18: Combined K-band degree of polarization and position angle are given here.

MWC 349: The interstellar degree of polarization and position angle values are taken from Yudin (1996) and are used to remove the interstellar contribution from observed polarization values of this star.

References

1) Hillenbrand et al. 1992; 2) Asselin, Manard and Bastien 1991; 3) Jain et al. 1995; 4) Oudmaijer et al. 2001; 5) Whittet et al. 1992; 6) Hutchinson et al. 1994; 7) Breger 1974; 8) Vrba et al. 1979; 9) Garrison and Anderson 1978; 10) Bastien 1982; 11) Bastien 1982; 12) Scarrott 1989; 13) Hall 1958; 14) Serkowski et al. 1975; 15) This paper 16) Yudin and Evans 1998; 17) Barbier and Swings 1992; 18) Gnedin et al. 1992; 19) Menard and Bastien 1992; 20) Vrba 1975; 21) Ward-Thompson et al. 1985; 22) Marrocco and Forte 1978 23) Draper et al. 1985; 24) Sato et al. 1985; 25) Yudin 1994; 26) Meyer et al. 2001; 27) Heiles 2000; 28) Manset and Bastien 2001; 29) Bessell and Eggen 1972.

**Table 4.** Relative orientations of binary, polarization and outflow position angles for Herbig Ae/Be stars.

| Object           | $ \Delta_{po} - 90 $<br>( $^{\circ}$ ) | $ \Delta_{bp} - 90 $<br>( $^{\circ}$ ) | $ \Delta_{bo} - 90 $<br>( $^{\circ}$ ) |
|------------------|--|--|--|
| V633 Cas         | 61                                     | 84                                     | 67                                     |
| V376 Cas         | 6                                      | -                                      | -                                      |
| XY Per           | -                                      | 41                                     | -                                      |
| V892 Tau         | -                                      | 70                                     | -                                      |
| UX Ori           | -                                      | 73                                     | -                                      |
| HD 35187         | -                                      | 50                                     | -                                      |
| CO Ori           | -                                      | 25                                     | -                                      |
| HK Ori           | 89                                     | 29                                     | 28                                     |
| T Ori            | -                                      | 63                                     | -                                      |
| V380 Ori         | 55,32                                  | 23                                     | 58,35                                  |
| LkH $\alpha$ 208 | 65                                     | 1                                      | 24                                     |
| GGD 18           | 21                                     | 83                                     | 14                                     |
| R Mon            | 1                                      | 30                                     | 61                                     |
| GU CMa           | -                                      | 70                                     | -                                      |
| Z CMa            | 23                                     | 40                                     | 27                                     |
| HD 53367         | -                                      | 13                                     | -                                      |
| NX Pup           | -                                      | 78                                     | -                                      |
| HD 76534         | -                                      | 81                                     | -                                      |
| Her 4636         | 76                                     | 38                                     | 24                                     |
| HD 141569        | -                                      | 47                                     | -                                      |
| HD 144432        | -                                      | 88                                     | -                                      |
| HR 5999          | -                                      | 84                                     | -                                      |
| HD 150193        | -                                      | 87                                     | -                                      |
| KK Oph           | -                                      | 23                                     | -                                      |
| HD 163296        | 28                                     | -                                      | -                                      |
| AS 310           | -                                      | -                                      | 8                                      |
| R CrA            | 31                                     | -                                      | -                                      |
| T CrA            | 42                                     | 4                                      | 52                                     |
| Par 21           | 10                                     | -                                      | -                                      |
| V1685 Cyg        | -                                      | 82                                     | -                                      |
| MWC 349          | 74                                     | 16                                     | 0                                      |
| LkH $\alpha$ 234 | 13,13                                  | 76                                     | 27,1                                   |
| PV Cep           | 2                                      | -                                      | -                                      |
| HD 200775        | 84                                     | 2                                      | 4                                      |
| AS 477           | 22                                     | 89                                     | 21                                     |
| LkH $\alpha$ 233 | 17,23                                  | -                                      | -                                      |
| HD 216629        | -                                      | 55                                     | -                                      |
| MWC 1080         | 0                                      | 26                                     | 64                                     |

median value of dispersion in position angle is  $\approx 8^{\circ}$ . Only for some stars namely, T Ori, HD 144432, AS 477 and MWC 1080, the dispersion in position angles is found to be more than or equal to  $30^{\circ}$ . Column 13 gives various apertures used in the polarimetric measurements and column 14 gives the references.

#### 4. Relationship between polarization angles, outflow directions and binary orbital planes

Various alignments between the linear polarization vector and other phenomena have earlier been looked for by several authors. The polarization vector is found to be perpendicular to the optical jets or CO molecular outflows for most sources (Mundt and Fried, 1983; Nagata, Sato and Kobayashi, 1983; Hodapp, 1984; Bastien, 1987). Bastien (1987) compiled a list of 23 young outflow sources for which the central source has been found and measured its linear polarization. The list included 8 TTS, 8 HAeBe, 1FUOR, 4 YSO, and 2 objects with unknown status. The distribution of the difference of the outflow position angle,  $\theta_{jet}$ , and the linear polarization position angle,  $\theta_*$ , was studied and it was found that in 61% of the sources these two directions are perpendicular to each other to within  $30^{\circ}$ . This was done to distinguish between two models of the origin of polarization namely oblate configuration as in a circumstellar disk around the star and prolate configuration as in two oppositely directed jets. Both the models have the same  $\sin^2 i$  dependence, and hence it is difficult to distinguish between elongated and flat models. However, the polarization is usually perpendicular to the scattering plane. One expects the polarization vector to be along the axis for flat models and perpendicular to it for the elongated distribution. Thus for an outflow source, the polarization vector and the outflow position angle would be roughly parallel to each other in a flat model and perpendicular to each other for an elongated model. Also, if the source is in a binary system and if the disk as well as the orbital plane are coplanar, the polarization position angle would be roughly perpendicular to the binary position angle in a flat model and parallel to the binary position angle in an elongated model (for favoured orientations). In the following we present a study of correlation between the binary, polarization and outflow position angles in Herbig Ae/Be stars.

In Table 4, the relative orientations of binary, polarization and outflow position angles are presented for individual stars. Columns in Table 4 give respectively, (1) object identification, (2)  $|\Delta_{po} - 90|$ , where  $\Delta_{po} = \theta_p - \theta_o \pm n\pi$ , (3)  $|\Delta_{bp} - 90|$ , where  $\Delta_{bp} = \theta_b - \theta_p \pm n\pi$ , (4)  $|\Delta_{bo} - 90|$ , where  $\Delta_{bo} = \theta_b - \theta_o \pm n\pi$ .  $\theta_b, \theta_p, \theta_o$  are the observed binary, polarization and outflow position angles respectively and  $\pi$  stands for  $180^{\circ}$ . In Table 4, 17 ( $\approx 85\%$ ) of the 20 outflow sources have outflow position angle within  $30^{\circ}$  of being either perpendicular or parallel to the polarization position angle. Histogram (a) shown in Figure 1 gives the frequency distribution of the difference in polarization and outflow position angles. Sources with outflow position angle within  $30^{\circ}$  of being perpendicular to polarization position angle ( $|\Delta_{po} - 90| \leq 30^{\circ}$ ) are found to be 55%. Polarization position angle can be perpendicular to outflow if the circumstellar disk is optically thick and the

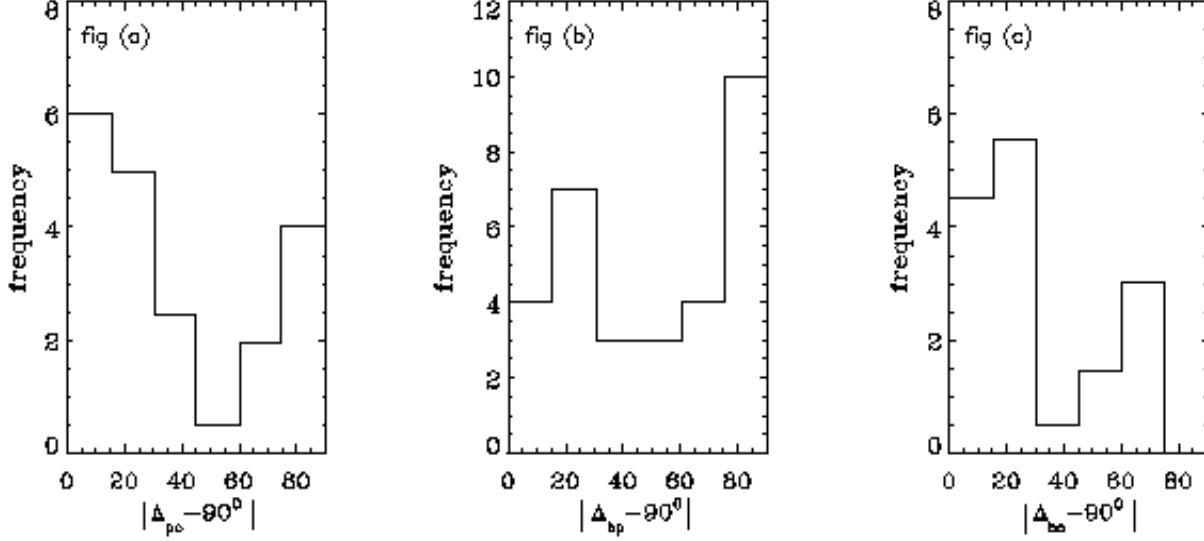


**Fig. 1.** Figure (a), the frequency distribution of the difference in polarization and outflow position angles. Figure (b), the frequency distribution of the difference in polarization and binary position angles. Figure (c), the frequency distribution of the difference in binary and outflow position angles.

outflow is perpendicular to it. As can be seen from Table 3, six sources, namely, V376 Cas, GGD 18, R Mon, Par 21, PV Cep and LkH $\alpha$  233 with polarization position angle perpendicular to outflow direction (within  $30^\circ$ ) have polarization value greater than 3%. This can happen when highly polarized scattered light from the optically thin polar regions superimposed on strongly attenuated unpolarized direct light from the central star reaches the observer whose line of sight is close to being edge-on. Five sources given in Table 3, namely, Z CMa, HD 163296, LkH $\alpha$  234, AS 477 and MWC 1080 with polarization position angle perpendicular to the outflow (within  $30^\circ$ ) have polarization value less than 3%. This situation can arise when polarized scattered light from the optically thin polar regions superimposed on weakly attenuated direct light from the central star reaches the observer whose line of sight is relatively away from the equatorial region. From Table 4, the sources with outflow position angle within  $30^\circ$  of being parallel to polarization position angle ( $|\Delta_{po} - 90^\circ| \geq 60^\circ$ ) are found to be 30%. Such a situation can arise when star has an oblate envelope or an optically thin disk. Sources satisfying this condition namely, V633 Cas, HK Ori, LkH $\alpha$  208, Her 4636 and HD 200775 have polarization values less than 3% except for MWC 349. Polarization values larger than  $\approx 2\%$  are hard to obtain owing to the presence of direct unpolarized light from the star and probably also because extremely oblate envelope do not occur (McLean & Brown, 1978). However, we note here that the interpretation in terms

of optically thin dust distribution may not be correct for some of these stars. Three of these stars (HK Ori, LkH $\alpha$  208 and HD 200775) were also studied by Hillenbrand et al. (1992) and were found to have Group I SEDs indicative of optically thick disks. Scattering off the surface of the optically thick disk (Whitney & Hartmann, 1992) may be responsible for the observed polarization for these objects. Among the 11 sources with polarization vectors perpendicular to the outflow, 7 are in common with Hillenbrand et al. (1992). Four of these (V376 Cas, R Mon, Par 21 and LkH $\alpha$  233) show Group II SEDs indicative of optically thick disks surrounded by extended envelopes, and 3 (HD 163296, LkH $\alpha$  234 and MWC 1080) show Group I SEDs. Three sources namely, V380 Ori, R CrA and T CrA have outflow position angle neither parallel nor perpendicular to the polarization position angle. This can happen when the outflow direction is not perpendicular to the circumstellar/circumbinary optically thin/thick disk. Fendt & Zinnecker (2000) showed that in some cases, protostellar jets and counter jets are misaligned and the reason they suggest for the misalignment is the bending of jets due to the motion of jet source in a binary system. Similar effects could be responsible for the outflow being neither perpendicular nor parallel to the polarization position angle in the binary systems V380 Ori and T CrA. R CrA is suggested to have an interstellar disk (Ward-Thompson et al. 1985) around it which bends the outflow originating from it. V380 Ori, LkH $\alpha$  234 and LkH $\alpha$  233 have outflows associated with

them in two directions. Each of them is counted 1/2 in the histogram. A two sided Kolmogorov-Smirnov test shows that the frequency distribution shown in Figure (a) is different from a random distribution to 97%. In Figure 2 the difference in polarization and outflow position angles ( $|\Delta_{po} - 90|$ ) is plotted against intrinsic polarization  $P_i$ . Error bars shown in Figure 2 result from probable errors in polarization measurements, uncertainties in the estimation for interstellar polarization, dispersions in multi-epoch values and the uncertainties in the outflow position angles. The probable errors in the outflow position angles are typically 5-20° (Bastien 1987) depending on the method of outflow detection (optical/NIR, radio) but are not given explicitly by the authors for most of the sources. Where not available, we have taken a value 5° for optical/NIR and 20° for radio observation. From Figure 2 it can be seen that objects with  $|\Delta_{po} - 90| \leq 30^\circ$  tend to exhibit large values of polarization indicative of optically thick disks with extended envelopes. These results strengthen the correlation found by Bastien (1987).

Histogram (b) in Figure 1 shows the frequency distribution of difference in polarization position angle and binary position angle. In Table 4, 25 ( $\approx 81\%$ ) out of 31 binary systems have polarization position angle within 30° of being either perpendicular or parallel to the binary position angle. Among 31 sources, 10 ( $\approx 32\%$ ) have polarization position angle within 15° of being parallel to the binary position angle while 45% of the sources show the two position angles parallel to within 30°. Parallelity of the two position angles can result if the binary component is coplanar with an optically thick disk since polarization arises due to the scattering of stellar light by the dust distributed in the polar regions. In 35% of the sources given in Table 4 polarization position angle is perpendicular to the binary position angle within 30°. This situation can arise when the binary component is coplanar with an optically thin disk where polarization arises due to the scattering of stellar light by the dust distributed in equatorial region. Alternatively, polarization could be caused by scattering off the surface of an optically thick disk (Whitney & Hartmann, 1992). A two sided Kolmogorov-Smirnov test shows that the frequency distribution shown in Figure (b) is different from a random distribution to 84%. However, the binary component position angle does not in a strict sense represent the orbital plane (except in edge-on systems) owing to the projection effects and this will weaken the correlation. We find here that there exists a correlation between binary position angle and polarization position angle inspite of the projection effect. This indicates that in actual case there exist a correlation that is even stronger than observed.

Histogram (c) in Figure 1 shows the frequency distribution of difference in binary and outflow position

angles. Among binary systems, there are 15 sources which are associated with outflows also. It can be seen that 10 ( $\approx 67\%$ ) of the 15 binary sources have the binary position angle within 30° of being perpendicular to outflow position angle. A two sided Kolmogorov-Smirnov test shows that the frequency distribution shown in Figure (c) is different from a random distribution to 96%. Here again it should be noted that the projection effects on the binary orbital planes would weaken even a perfect correlation (perpendicularity) between the outflow and binary position angles. So the observed correlation is relatively more significant.

The results presented in Figure 1, the various correlations and their interpretation discussed above must be viewed with caution as they are based on relatively small number statistics (17/20, 25/31, 10/15). In particular, for the restricted sample of binary sources with outflows, only 7 ( $\approx 50\%$ ) are compatible with the interpretation of their polarization position angle relative to the outflow and binary position angles. Also, projection effects on binary orbital planes, as noted earlier, tend to reduce the observed correlations. Correlations between the different position angle differences and binary component separation were also investigated. For  $|\Delta_{po} - 90|$ ,  $|\Delta_{bp} - 90|$  and  $|\Delta_{bo} - 90|$  as a function of log (projected linear separation in AU) we obtain very low linear correlation coefficients (0.26, 0.17, 0.20 respectively) indicating poor correlation.

## 5. Discussion

The geometrical relationships between binary position angle, polarization position angle and outflow position angle studied here can be compared with those expected from different mechanisms of formation of binary system, circumstellar disks and young stellar objects. The favoured binary formation mechanisms are: (1) capture process - in which two independently formed stars can be captured into orbits under certain conditions (Hills 1976; Boss 1988; Hills & Day 1976; Mansbach 1970); (2) fission process - in which as a star contracts towards mainsequence it spins up and the ratio of rotational to gravitational energy ( $\beta$ ) increases. When ( $\beta$ ) increases beyond a certain critical value, the star becomes unstable to non-axisymmetric perturbations. It has been hypothesized that breakup into orbiting subcondensations then occurs (Ruzmaikina 1981a,b; Williams & Tohline 1988); (3) fragmentation - in which a cloud that is initially differentially rotating (Myhill & Kaula 1991), or has a milder exponential-type density profile (Boss 1991), fragments. Another mode of fragmentation was suggested by Zinnecker (1990) where he proposed that since most of the interstellar clouds often show an elongated, filamentary structure, it rotates about an axis perpendicular to the cylindrical axis. After fragmentation of the cylinder (Bastien 1983) the fragments move towards each other along the cylindrical



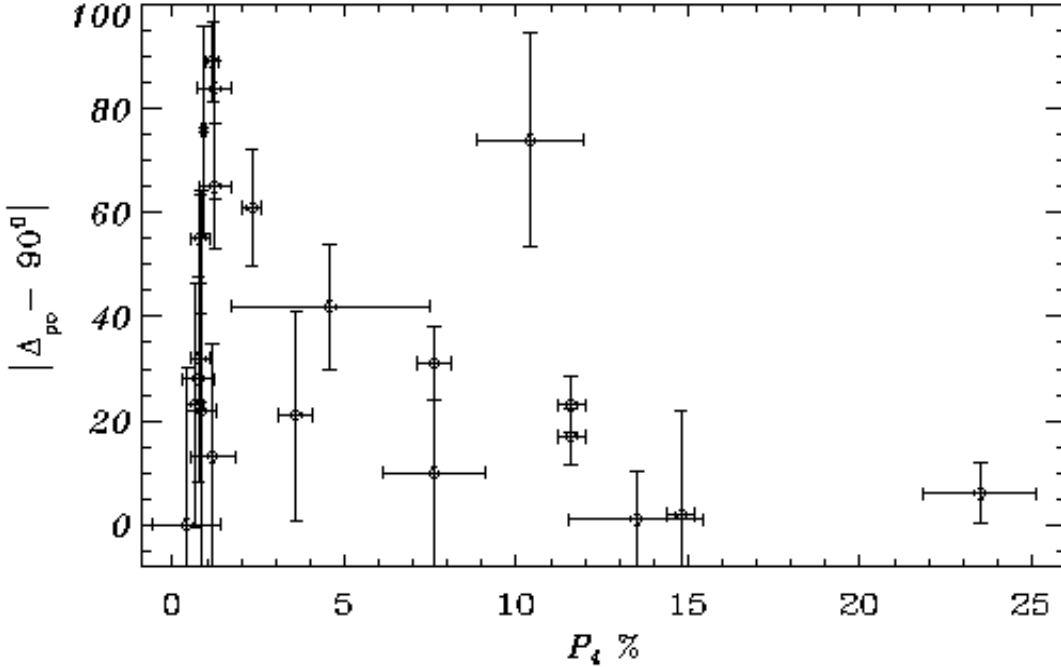


**Fig. 2.** Difference in polarization and outflow position angles plotted against intrinsic polarization  $P_i$ .

axis until they reach a Keplerian orbit. This mechanism results in the formation of binary systems with wide separation; (4) disk fragmentation - in which a relatively slowly rotating protostar collapses through the adiabatic phase without fragmentation and will form a disk-like structure. Equilibrium Keplerian disks around central stars have the possibility of fragmenting due to gravitational instabilities (Adams, Ruden & Shu 1989; Shu et al. 1990). In all the above mentioned binary formation mechanisms except the capture, one would expect the disk around each component or the circumbinary disk and the binary orbit to be coplanar. Results presented in this paper support those binary formation mechanisms in which disk around each component or circumbinary disk and the binary orbital plane are coplanar. While polarization position angle could be either parallel or perpendicular to the circumstellar disk depending on the optical depth and the presence of extended envelopes, the outflow direction is expected to be always perpendicular to the disk. If the disks are coplanar with binary orbital plane, then the outflow position angle should be perpendicular to the binary position angle except for any projection effect. From Figure 3 it is seen that out of 15 outflows listed here 10 of them have difference in binary component and outflow to be within  $30^\circ$  of

being perpendicular to each other. The polarimetric observations used in this work have generally been made with large apertures ( $\approx 10 - 15 \text{ arcsec}$ ) encompassing both the components of the Herbig Ae/Be binaries (with typical angular separation of  $\leq 2 \text{ arcsec}$ ). Since the optical light is dominated by the primary component the observed polarization is determined by the distribution of scattering matter around it. The outflow in a binary Herbig Ae/Be star could be driven by either the primary or even the secondary which is generally a low mass infrared object, having its own circumstellar disk. The results on the correlations between the various position angles discussed above therefore indicate coplanarity of the disks around the individual components. For low mass T Tauri binaries, polarimetry on individual component stars (Jensen et al. 2000; Wolf et al. 2001 and Monin et al. 2000) have shown that in a majority of the binary systems the linear polarization vectors from individual stars are within  $30^\circ$  of being parallel. Resolved polarimetric measurements of the Herbig Ae/Be binary components will be needed to confirm the results presented here.

## 6. Conclusions

Circumstellar matter around Herbig Ae/Be stars causes polarization in the light from these objects due to scattering from dust. The position angle of the observed polarization depends on whether the scattering is dominated by optically thin disk or by optically thin/thick scattering dust distributed perpendicularly to an optically thick disk. Bipolar outflows are generally constrained to be perpendicular to the disks. In binary Herbig Ae/Be stars, the binary orbital plane may also be correlated with the polarization and outflow directions if the binary formation mechanism derives the binary orbital angular momentum and the individual star's circumstellar disk from the angular momentum of the same rotating clouds. In this paper we have studied the observed correlation between the different position angles. Our results can be summarized as follows:

1) Out of 20 outflow sources, 17 sources ( $\approx 85\%$ ) have the outflow position angle within  $30^\circ$  of being either parallel or perpendicular to the polarization position angle.

2) In 25 ( $\approx 81\%$ ) out of 31 sources, the direction of binary position angle is within  $30^\circ$  of being either parallel or perpendicular to the polarization position angle.

3) In 10 ( $\approx 67\%$ ) out of 15 outflow sources, the binary position angle is within  $30^\circ$  of being perpendicular to the outflow position angle.

These results are consistent with binary star formation scenarios in which the circumstellar disk planes are parallel to the binary orbital plane. However, it must be noted that these results are subject to small number statistics as they are based on samples that are small and need to be enlarged.

*Acknowledgements.* We thank the referee for valuable comments that have led to substantial improvements in the analysis and presentation of the paper.

## References

- Adams, F. C., Emerson J. P., & Fuller G. A., 1990, ApJ 357, 606
- Adams, F. C., Ruden, S. P., Shu, F. H., 1989, ApJ 347, 959
- Ageorges, N., Eckart, A., Monin, J. -L., Menard, F., 1997, A&A 326, 632
- Asselin, L., Menard, F., Bastien, P., 1996, ApJ 472, 349
- Bailey, J., 1998, MNRAS 301, 161
- Barbier, R., Swings, J. P., 1982, IAUS 98, 103
- Bastien, P., 1982, A&AS 48, 159
- Bastien, P., 1982, ApJS 59, 277
- Bastien, P., 1983, A&A 119, 109
- Bastien, P., 1987, ApJ 317, 231
- Beckwith, S. V. W., Sargent, A. I., Chini, R. S. & Gusten, R. 1990, AJ 99, 924
- Berrilli, F., Corciulo, G., Ingrassio, G. et al., 1992, ApJ 398, 254
- Bertout, C., Basri, G. & Bouvier, J., 1988, ApJ 330, 350
- Bertout, C., Robichon, N., Arenou, F., 1999, A&A 352, 574
- Bessell and Eggen, 1972, ApJ 177, 209
- Boss, A. P., 1988, ComAp 12, 169
- Boss, A. P., 1991, Nature 351, 298
- Brandner, W., Bouvier J., Grebel E. K., et al., 1995, A&A 298, 818
- Breger, M., 1974, ApJ 188, 53
- Brown, J. C., & McLean I. S., 1977, A&A 57, 141
- Cabrit, S., Lagage, P. -O., McCaughrean, M., Olofsson, G., 1997 A&A 321, 523
- Canto, J., Rodriguez, L. F., Calvet, N., Levreault, R.M., 1984, ApJ 282, 631
- Chelli, A., Cruz-Gonzalez I., Reipurth B., 1995 A&As 114, 135
- Close, L. M., Roddier, F., Hora J. L., et al., 1997, ApJ 489, 210
- Cohen, M., Kuhl, L. V., 1979, ApJS 41, 743
- Corcoran, M. & Ray, T. P., 1998, A&A 336, 538
- Devine, D., Grady, C. A., Kimble, R. A., et al., 2000, ApJ 542, L115
- Dommanget J., Nys O., 1994, CoORB(Components of Double and Multiple stars,CCDM ) 115, 1D
- Draper, P. W., Warren-Smith, R. F., Scarrott, S. M., 1985, MNRAS 212 P1
- Dunkin, S. K., Crawford, I. A., 1998, MNRAS 298, 275
- Elsasser, H. & Staude, H. J., 1978, A&A 70, L3
- Fendt, C., Zinnecker, H., 2000, IAUS 200, 112
- Finkenzeller, U., Mundt, R., 1984, A&AS 55, 109
- Garrison, L. M. & Anderson, C. M., 1978, ApJ 221, 601
- Gnedin, Y. N., Kiselev, N. N., Pogodin, M. A., Rozenbush, A. E., Rozenbush, V. K., 1992, SvAL 18, 182
- Goodrich, R. W., 1993, ApJS 86, 499
- Hall, J. S., Pub. U.S.Naval Obs. 17/VI
- Herbig, G. H., 1960, ApJS 4, 337
- Heiles, C., 2000, AJ 119, 923
- Hillenbrand, L. A., Strom, S.E., Vrba, F. J. & Keene, J., 1992, ApJ 397, 613
- Hills, J. G., 1976, MNRAS 175, 1
- Hills, J. G., and Day, C. A., 1976, ApL 17, 87
- Hodapp, K. -W., 1984, A&A 141, 255
- Hsu, J. C. & Breger, M., 1982, ApJ 262, 732
- Hutchinson, M. G., Albinson, J. S., Barrett, P., et al. 1994 A&A 285, 883
- Jain, S. K., Bhatt, H. C. & Sagar R., 1990, A&AS 83, 237
- Jain, S. K. & Bhatt, H. C., 1995, A&AS 111, 399
- Jain, S. K. & Srinivasulu, G., 1991, opt. Eng. 30, 1415
- Jensen, Eric, L. N., Donar, Arianne X., Mathieu, Robert D., 2000, IAUS 200, 85
- Konigl, A., 1982, ApJ 261, 115
- Lada, C. J., Gautier, T. N., 1982 ApJ 261, 161
- Larson, R. B., 1990, in Physical processes in fragmentation and star formation, eds. R. Capuzzo-Dolcetta et al., Kluwer, Dordrecht 389
- Leinert, C., Richichi A., Haas M., 1997, A&A 318, 472
- Lenzen, R., Hodapp, K. -W., Reddmann, T., 1984, A&A 137, 365

- Mansbach, P., 1970, ApJ 160, 135
- Manset, N., Bastien, P., 2000, AJ 120, 413
- Marraco, H. G., Forte, J. C., 1978 ApJ 224, 473
- McLean, I. S., Brown, J. C., 1978 A&A 69, 291
- Menard, F., Bastien, P., 1992, AJ 103, 564
- Meyer, M. J., Nordsieck, K. H., Hoffman, J. L., 2001, accepted in AJ.
- Monin, J.-L., Menard, F., Peretto, N., 2001, The Messenger 104, 29
- Mundt, R., and Fried, J. W., 1983, ApJ 274, L83
- Myhill, E. M., Kaula, W. M., In NASA, Washington, Reports of Planetary Geology and Geophysics Program, 1990, 420
- Nagata, T., Sato, S., Kobayashi, Y., 1983, A&A 119, L1
- Natta, A., Palla, F., Butner, H.M., et al., 1993, ApJ 406, 674
- Oudmaijer, R. D., Palacios, J., Eiroa, C., et al., 2001, A&A 379, 564
- Palla, F., Stahler S. W., 1991, ApJ 375, 288
- Pirzkal, N., Spillar, E. J., Dyck, H. M., 1997, ApJ 481, 392
- Poetzel, R., Mundt, R., Ray, T. P., 1989, A&A 224, L13
- Poetzel, R., Mundt, R., Ray, T. P., 1992, A&A 262, 229
- Ray, T. P., Poetzel, R., Solf, J., 1990, ApJ 357, L45
- Reipurth, Bo., Bally, J., Devine, D., 1997, AJ 114, 2708
- Ruzmaikina, T.V., 1981a, Adv. Space Res. 1, No 7, 49
- Ruzmaikina, T.V., 1981b, Pisma Astr. J. U.S.S.R. 7, 188
- Rydgren, A.E., Strom, S. E. & Strom K.E., 1976, ApJS 30, 307
- Sato, S., Nagata, T., Nakajima, T., et al., 1985, ApJ 291, 708
- Scarrott, S. M. Draper, P. W., Warren-Smith, R. F., 1989 MNRAS 237, 621
- Serkowski, K., 1974, in Planets, Stars and Nebulae studied with photopolarimetry, ed. T. Gehrels, Univ. Arizona Press, Tucson 135
- Serkowski, K., Mathewson, D. S., Ford, V. L., 1975, ApJ 196, 261
- Shu, F.H., Tremaine, S., Adams, F.C., and Ruden, S.P., 1990, ApJ 358, 495
- Strom, K. M., Strom, S. E., Kenyon S. J. & Hartmann L., 1988, AJ 95, 534
- Strom, K. M., Strom, S. E., Wolff S. C., Morgan J. & Wenz M., 1986, ApJS 62, 39
- Strom, S. E., Strom, K. M., Yost J. Carrasco L., Grasdalen G., 1972, ApJ 173, 353
- Thé, P. S., de Winter D., Pe'rez M.R. 1994, A&AS 104, 315
- van den Ancker, M.E., de Winter, D., Tjin A Djie, H. R. E., 1998, A&A 330, 145
- Vrba, F. J., 1975, ApJ 195, 101
- Vrba, F. J., Schmidt, G. D., Hintzen, P. M., 1979, ApJ 227, 185
- Ward-Thomson, W. D., Warren-Smith, R. F., Scarrott, S. M., 1985, MNRAS 215, 537
- Watt, G. D., Burton, W. B., Choe, S. U., Liszt, H. S., 1986, A&A 163, 194
- Weintraub, D. A., Sadnell G. & Duncan W.D., 1989 ApJ 340, L69
- White, G. J., 1993, A&A 274, L33
- White, R. L., Becker, R. H., 1985 ApJ 297, 677
- Whittet, D. C. B., Martin, P. G., Hough, J. H., et al., 1992, ApJ 386, 562
- Whitney, B. A., Hartmann Lee, 1992, ApJ 395, 529
- Whitney, B. A., Hartmann Lee, 1993, ApJ 402, 605
- Williams, P. M., Brand P. W. J. L., Longmore A. J, et al. 1977, MNRAS 180, 709
- Williams, H. A., and Tohline, J. E., 1988, ApJ 334, 449
- Wolf, S., Stecklum, B., Henning, Th., 2001. IAU 200, 295
- Yudin, R., 1994, ASP con. 62, 82
- Yudin, R. V., 1996, A&A 312, 234
- Yudin, R. V. & Evans A., 1998, A&AS 131, 401
- Zinnecker, H., 1990, in Low Mass Star Formation and Pre-Main-Sequence objects, ed. B. Reipurth, 447